New polarized neutron diffraction setup for precise high-field investigations of magnetic structures up to 8 T at MLZ

Vladimir Hutanu[1,2], Henrik Thoma[1,2], Hao Deng[1,2], Georg Brandl[2], Alexander Weber[2], Valentyn Rubanskyi[2], Jürgen Peters[3]; Wolfgang Luberstetter[1,2], Thomas Krist[4], Georg Roth[1], Lars Peters[1], Thomas Brückel[5], Stefan Mattauch[2]

[1]Institute of Crystallography RWTH Aachen University, D52066 Aachen, Germany

[2]Jülich Centre for Neutron Science JCNS at Heinz Maier-Leibnitz Zentrum (MLZ), Forschungszentrum Julich GmbH, Germany

[3]Forschungs-Neutronenquelle Heinz Maier-Leibnitz (FRM II), D85747 Garching b. München, Germany

[4]NOB Nano Optics Berlin GmbH, Krumme Str. 64, D10627 Berlin, Germany

[5]Juelich Centre for Neutron Science JCNS and Peter Gruenberg Institut PGI JCNS-2 & PGI-4, Forschungszentrum Juelich GmbH, Jülich, Germany.

Index Terms— High magnetic field, magnetic structure, polarized neutron diffraction, supermirror polarizer.

New actively shielded asymmetric vertical field split-coil superconducting magnet with maximal field of 8 T has been recently procured and implemented on the beam line POLI at Maier-Leibnitz Zentrum (MLZ). The magnet is designed in order to facilitate the single crystal diffraction with polarised neutrons. In order to provide high neutron polarisation in the vicinity of the new strong magnet a dedicated compact-size solid-state supermirror bender polariser optimised for the short neutron wavelength on POLI has been built. A Mezei flipper, which had been previously developed for lower field, could be upgraded with additional guide fields in order to be used in combination with new polarizer and magnet. All components are discussed and the performance test for the entire setup is presented. High efficiency of the new polarised neutron diffraction setup on POLI is demonstrated. Polarized neutron diffraction experiments in the fields up to 8 T are now available at MLZ.

I INTRODUCTION

Polarized neutron diffraction (PND) is a powerful method for investigating magnetic structures. It gives unique access to contributions from nuclear and magnetic scattering, their interference terms, magnetic chirality, and permits to discriminate between them. In contrast to non-polarized neutron diffraction, where the scattered intensity depends on the square of the magnetic structure factor, PND has a linear nuclear–magnetic interference term as part of the scattered intensity. This increases the precision in the determination of small ordered magnetic moments by at least one order of magnitude. In classical PND, the sample is situated in a strong magnetic field. For each Bragg reflection, two scattered cross sections are measured for the two antiparallel polarizations of the incoming neutron beam, and the ratio between them is built [1]. PND measurements are used for the refinement of magnetization density distribution maps [2,3] and the determination of local anisotropy in the

magnetic susceptibility at the unit-cell level [4]. It is also used for the high-quality determination of magnetic form factors [5,6], to untangle complex (e.g. chiral) magnetic structures and to follow the movement of magnetic domains [7,8]. Recently demonstrated application of PND to the determination of the absolute sign of the Dzyaloshinskii-Moriya interaction in bulk non-centrosymmetric antiferromagnets [9] opens new perspectives for this classical method e.g for the studies in the antiferromagnetic spintronics.

Recently, a first PND setup using a compact high T_c superconducting magnet and a ^{3}He spin filter neutron polarizer has been successfully implemented [10,11] on the hot neutrons single crystal diffractometer POLI at Heinz Maier-Leibnitz Zentrum (MLZ) in Garching near Munich, Germany [12]. Although this setup performs well and first scientific output from it starts to appear e.g. [2,8], it suffers from the relatively low maximal available field of only 2.2 T. For studying many topical magnetic materials with small ordered magnetic moment e.g., quantum-, topological-, complex frustrated-magnets, the field-limit of about 2 T is insufficient to produce significant measurable signal, even for PND. To overcome this limitation, a new 8 T split-coil superconducting magnet has been procured and implemented for measurements on POLI. In the following we will present the advantages of the new magnet and its implementation for PND on POLI. A number of the new instrumental components have been designed, produced and tested. Their performance as well as the installation and the overall performance check for the whole instrument are presented in this report.

II. MAIN COMPONENTS OF THE PND SETUP

A. New split-coil 8 T superconducting magnet

Liquid He bath cryostat-based, vertical field split-coil magnets using "classical" Nb_3Sn and NbTi superconductors became in the last decades a standard device for magnetic neutron scattering (diffraction and spectroscopy) in most neutron facilities over the world. The typical maximal field values in the neutron path on such devices reaches 5-10 T (up to 14-16 T in some large prototypes). The field range is limited by the intrinsic properties of the used superconductor and the magnet design. Usually, limitations like the available opening angle for the neutron beam (both in vertical and horizontal directions), clearance between the coils (sample height), sample space diameter, field homogeneity, but also maximal weight of the device or overall available size in the beam path, as well as maximal allowed fringe field values lead to the compromises in reaching the highest possible field value. In this regard, the new 8 T magnet produced by Oxford Instrument Inc. for neutron scattering at MLZ was subject of thorough design-optimisation in order to satisfy all requirements especially for the polarised single crystal neutron diffraction, but also for the other applications. It provides a large angular acceptance for the scattered beam of 300° in the horizontal and 30° (-5°/+25°) in the vertical plane, respectively, permitting both a right- and left-handed scattering geometry, the registering of the out-of-plane reflections and the usage of large 2D detectors. The field polarity can be swiped between positive and negative. The vertical asymmetric field configuration is realized as the standard operation mode to shift the zero-field node between the direct and fringe field out of the incoming beam path to avoid a neutron depolarization. The magnet is equipped with a re-condensing liquid He cryostat using a Joule-Thomson cold head on top to liquefy the exhaust He gas back into the cryogen bath, same as in the prototype described by Kirichek at al. [13]. Under a constant temperature condition, a zero He boil-off rate could be maintained over a long time (weeks or even month). This significantly reduces the operation costs and maintenance effort for the regular refilling during the neutron experiments. Using two sample rods with dedicated thermometry, sample temperatures between 1.7 and 800 K are available. An extension to the mK range is planned, using an additional ^{3}He/^{4}He dilution insert. The sample rod is equipped with an automated axial rotation and a vertical

translation for precise sample centring and diffraction measurements. The spacious sample tube (Ø=34 mm) and large coil-split size of 53 mm facilitates multi-parameter studies by fitting inside e.g. a pressure cell [14] or other equipment like micro positioners, laser fibres, etc. The installation of high-voltage lines for an additional electric field at the sample position is ongoing. Selected technical characteristics of the new asymmetric-field 8 T magnet are presented in Table 1. A photograph of the magnet mounted on the sample table of instrument POLI is shown in the Figure 1.

TABLE I

Selected technical characteristics of the new 8 T magnet at MLZ

Specification	**Value**
Max. central flux density in normal operation at 4.2 K	+/- 8 T
Minimal relative flux density homogeneity over transverse cylinder 10 mm diam. x 10 mm long	0.42 %
Stray magnetic field 1 m in the axial direction below the magnet 1 m in the radial direction at mid plane	 24 Oe 25 Oe
Flux density temporal stability	0.0006% h^{-1}
Maximum sweep rate	0.27 T min^{-1}
Energisation time to max. field	~ 30 min
Neutron window material thickness	10 mm Al alloy
Low temperature sample rod range	1.4 – 400 K
High temperature sample rod range	40 – 800 K
Max diameter of the top flange	780 mm
Tail diameter at neutron window	600 mm
System weight including cryogens	740 kg
Cool down time using 260 l liquid He	< 48 h
Cryogen autonomy in the steady state re-condensing conditions	Unlimited

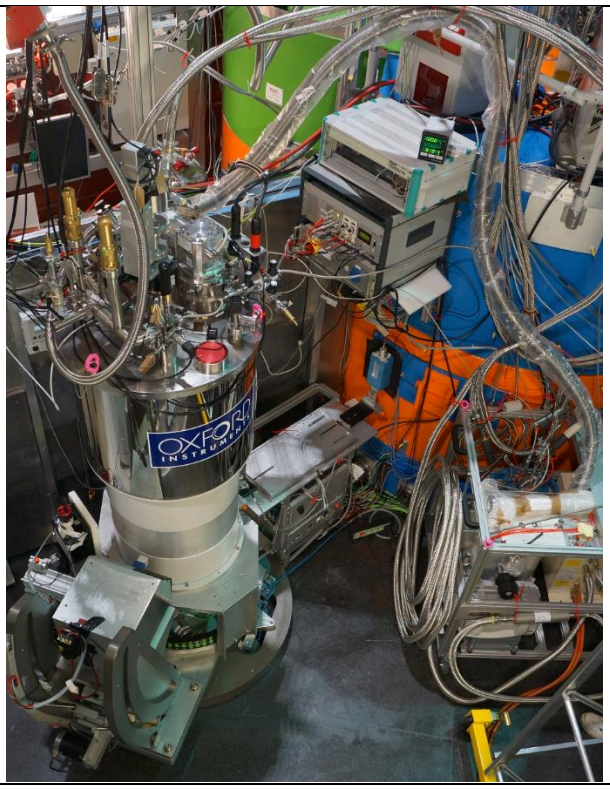

Fig. 1 Top view on the 8 T magnet installed on the sample table POLI. On the right side in the picture is the auxiliary equipment trolley containing vacuum pump, liquid N_2 trap and He compressor connected to the top flange of the re-condensing cryostat. The controls for the magnet - power supplies, electronics, cryogen level meters, temperature, field, motor stages control for the sample rod, security sensors etc. - are all placed in an additional air-cooled electronics rack (not shown here).

B. Supermirror bender polarizer

Although the new magnet is actively shielded, reducing the stray field by an order of magnitude compared to the classical design (25 Oe at 1 m radial distance from the magnets centre), its fringe fields gradients are still too large to be used with the sensitive ^{3}He polarizer of the previous setup [11]. To overcome this issue, a new large-beam-cross-section (130 x 42 mm^2) solid-state supermirror bender polarizer has been developed for POLI. It can be employed because the stray field of the magnet used as guide field for the neutron polarization, is in the same direction as, and smaller than, the field of the bender. As the bender's field strength is clearly above 500 Oe, its polarizing efficiency is not sensitive to the gradients of the magnet's stray field. The strong NdFeB-type permanent magnets creating the bender's field are arranged in H-configuration which leads to the same field direction inside and outside of the bender, thus avoiding a field reversal in the flight path of the neutrons. The bender consists of a stack of thin Si wafers coated on both sides with Fe/Si supermirrors with m=3. Additional Gd layers are deposited on both sides of each wafer to absorb the wrong spin component. The bending radius is optimised for the short wavelengths used on POLI to provide at least one reflection inside the thin Si channel. The total deflection of the polarised beam in comparison to the incoming "straight" beam is only about 0.4°. Taking into account the short distance between the polarizer and the sample on POLI (~ 1 m), only a small shift of a few millimetres is produced for the polarised beam on the sample position. This can be easily compensated by motorised translation and rotation stages. The whole bender was produced by the company NOB [15]. At neutron wavelengths of around 1 Å intensity losses due to Bragg scattering from the Si are considerable. Therefore, the width of the wafers and the length

of the bender (140 mm) should be as small as possible. On the other hand, the supermirror coating should not have a too high critical angle, which strongly increases the incoming divergence und thus reduces the amount of usable neutrons. As a compromise, the value of m=3 was chosen as optimal for the single crystal diffraction on relatively small samples (few mm size). It is an important advantage of such a small polarizer that the radiation due to the absorption of the wrong spin component can be shielded in a similarly small volume and thus, with limited weight also improving the peak/background ratio. The polarizer acts as an additional collimator for the incoming beam further reducing the background. The polarizing efficiency and transmission of the bender and their homogeneity over the beam cross section have been exhaustively tested using a small perfect Heusler crystal analyser as described in detail in the next section. A very high polarising efficiency for both standardly used short wavelengths on POLI could be reached (Fig. 2). No significant wavelength dependence in polarization is observed. The polarization is homogeneous over the transversal bender cross section. However, a somehow inhomogeneous transmission could be registered. As the transversal bender size with 42 mm is clearly larger than the typical studied sample size of < 10 mm, it is possible to use only the best performing portion of the bender/beam. Therefore, its optimised position concerning the beam source and sample was determined. The optimised transmission values for the correct spin component of about 18.2% for 1.15 Å and about 15.5% for 0.9 Å were determined. This is lower than the theoretically expected value based solely on the Si absorption by a factor of about 1.5-1.7 and might be attributed to the randomisation of the orientation of the single wavers to each other in order to avoid substantial Bragg reflection in the bulk of the Si body. This practice, which proved to be beneficial for cold neutrons, seems however to be less useful for shorter wavelengths.

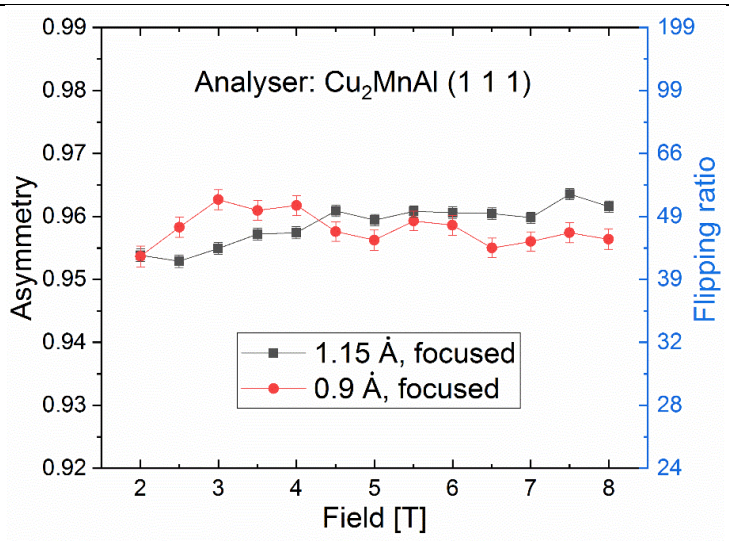

Fig. 2 Flipping ratio and polarization asymmetry measured with two standard wavelengths on POLI using a small perfect Heusler crystal analyzer.

C. Guiding and flipping neutron polarization

The overall performance of a PND setup is determined not only by the polarization efficiency of the polarizer, but also by the polarization transport efficiency as well. The latter one includes both the polarization losses by the guide fields and inside the magnet, but also the flipping efficiency of the used flipper between the polarizer and the sample. An efficient transport and flip of the neutron polarization is more difficult to provide for hot neutrons in comparison to thermal and cold ones as stronger guiding fields are necessary. An efficient shielded Mezei-type flipper has been developed on POLI for a 2.2 T magnet setup (Fig. 3 top left). Its design advantages and drawbacks as well as the technical realisation

is discussed elsewhere in detail [10, 11]. An attempt to use this existing flipper also in combination with the new bender polarizer and the 8 T magnet has been made. On one side, one observed a reasonably good performance of the non-focussed neutron beam as the sample reflects only the central portion of the whole incoming spot. On the other side, a significant dependence of the reached overall polarization degree from the used monochromator focusing could be observed. This is caused by some partial beam depolarization in the edge regions by the field inhomogeneities shown by the red vortices in Fig. 3, top left. To prevent such depolarization and extend the accepted field region for the efficient flipper operation, a dedicated guide-field construction was numerically simulated, optimized and built, to link the magnetic field of the bender to the flipper and to the stray field of the magnet (Fig. 3 top right). The position of the flipper in regard to the magnet and polarizer was also numerically optimised as shown in the Fig. 3 bottom left. The old flipper with the new guide field segments could be successfully calibrated in dependence on the main field in the magnet. The experimental calibration curves are shown in the Fig. 3 bottom right. It is easy to observe that the flipping current (black symbols in the figure), which should only be dependent on the used neutron wavelength, remains almost constant over the whole field region between 0-8 T. This shows that the flipping coil is well screened from the stray fields of the magnet by the compensation coil. In contrast to that, the current in the compensation coil (red symbols in the figure) is monotonically increasing with increasing field in the magnet and subsequently increasing stray field at the flipper position. Such smooth and predictable variation (no jumps or anomalies) correspond to the expectations and calculated values, denoting a reliable high flipping efficiency operation within the entire available field region.

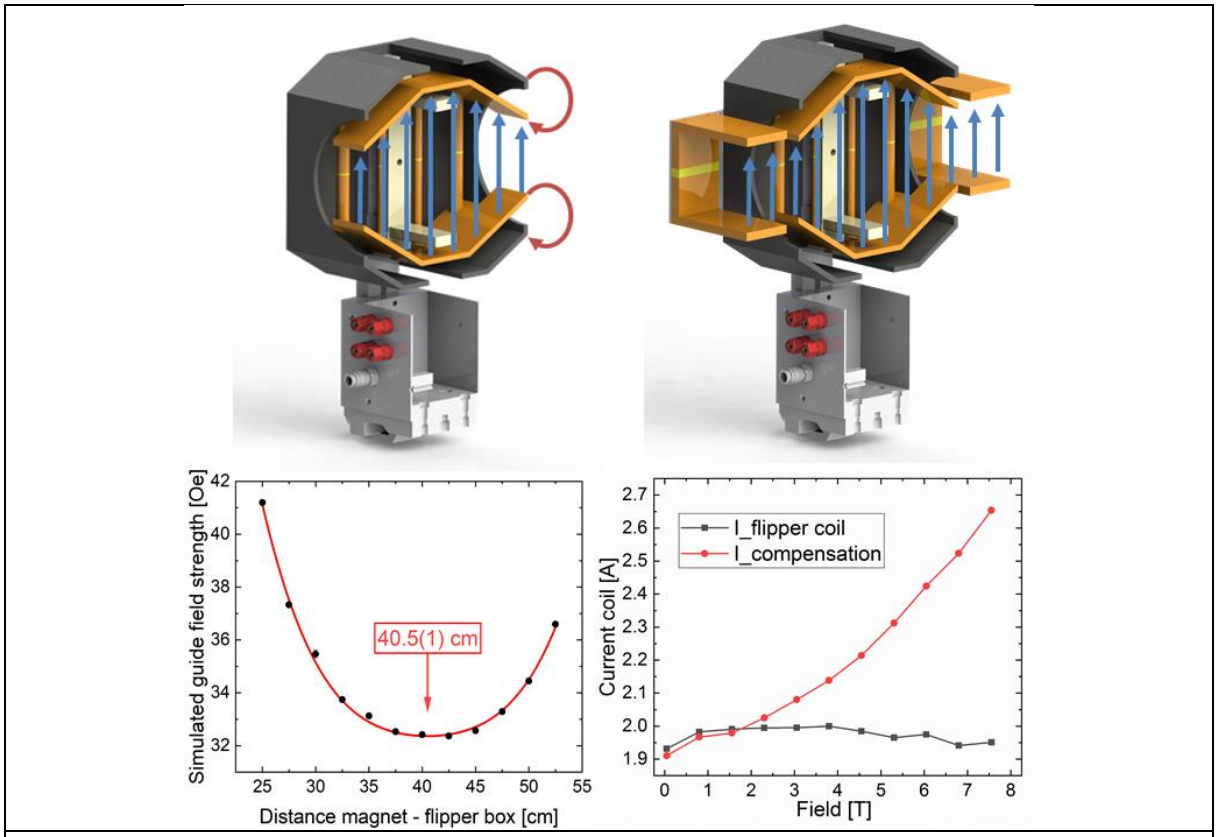

Fig. 3 Magnetic design of the shielded Mezei flipper. *Top left*: Previous design developed for the symmetric field 2.2 T magnet discussed in Ref. [10, 11]. Additional depolarization will occur on the edges denoted by the red arrows. *Top right:* Modified design with additional polar pieces (orange) and permanent magnets (yellow) to avoid field vortices. *Bottom left:* Numeric optimisation of the flipper position with respect to the magnet. *Bottom right:* Experimental flipper-coils calibration as function of the field in the magnet.

Figure 4 shows the neutron beam path between the monochromator-drum and the sample in the magnet. The non-polarised horizontally and vertically focused monochromatic neutron beam with a short wavelength of 0.9 or 1.15 Å is coming from the right side of the picture (red arrow). It passes an erbium λ/2 filter and an incoming monitor before entering the bender polarizer. The bender is situated on motorised translation stage, which allows movement transversal to the beam. This permits easy positioning in or moving out of the beam for polarized/non polarised measurements, respectively. The polarized neutrons are propagating in the vertical guide field produced by bender, flipper and stray fields of the magnet. The beam is shaped by the slits before the sample/magnet to optimise the signal/background ratio. Up (+) /Down (-) polarization of the incoming beam is controlled by the current in the flipper coils.

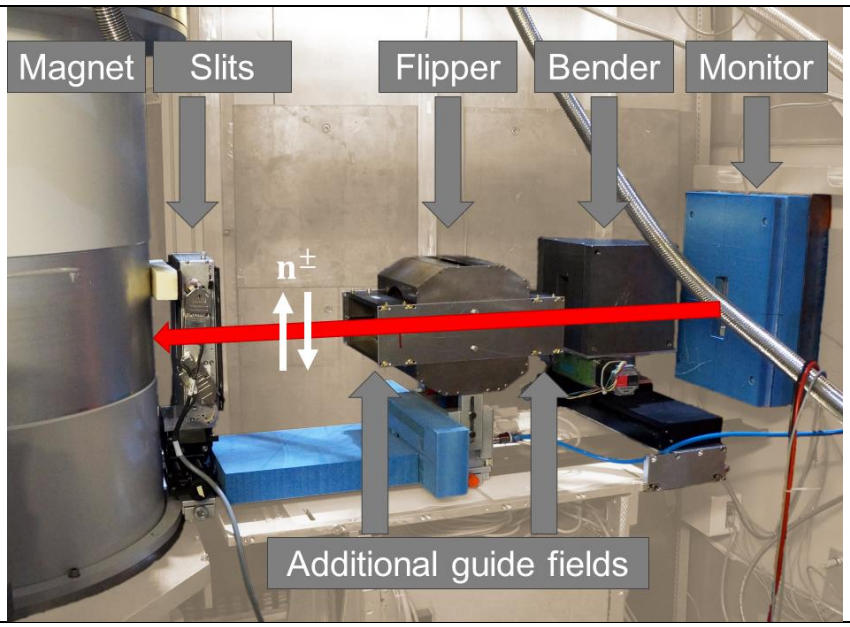

Fig. 4 Components of the PND setup on POLI along the incoming neutron path.

III PERFORMANCE TEST RESULTS

In PND not the absolute intensity of the Bragg reflections (like in traditional diffraction) is measured, but so-called flipping ratio (FR) FR = I^+/I^- , or equivalent the polarization asymmetry A = $(I^+ - I^-) / (I^+ + I^-)$. Here $I^\pm$ denotes the measured intensity for the two antiparallel polarizations of the incoming neutron beam in regard to the quantization axis of the field. Using a polarization analyzer with determined efficiency and a purely nuclear Bragg reflection, the experimentally measured asymmetry gives direct access to the polarization transport and polarizer efficiency.

$$\frac{I^+ - I^-}{I^+ + I^-} = P_{Pol}\, P_{An}\, P_T \qquad (1)$$

Here I^+ and I^- are the counting rates obtained with deactivated and activated flipper, respectively. P_{Pol} and P_{An}, are polarizing and analyzing efficiencies, respectively. P_T is the polarized neutron spin transport efficiency accounting for all setup-related losses and the flipping efficiency. Since there is no magnetic contribution to the nuclear peak, the spin state is conserved during the scattering process. Thus, the polarization before and after the sample remains the same and only setup-related effects influence the measurement. The Decpol analyzer with the ^{3}He spin filter cell (SFC) described in Ref.

[16] was used to prove the setup efficiency in the low-field region (< 1 T). By measuring the transmission of a non-polarized neutron beam, P_{An} can be determined precisely, for example using the formulae presented in Ref. [17], where typical SFCs used on POLI are also described. In our measurement, the nuclear (220) reflection of a Cu single-crystal sample was used. The resulting P_{Pol} P_T obtained from the measured asymmetry by normalizing for the efficiency of the used SFC is shown in Fig. 5 with red symbols. Using optimised flipper currents, the asymmetries for all fields between 0.05 and 1 T with 0.1 T step were measured. A constantly high P_{Pol} P_T value of > 99% is observed. At higher fields ^{3}He SFC may depolarize, therefore a Heusler (Cu_2MnAl) single-crystal sample situated in the magnet was used as analyzer. For the (111) reflection of the Heusler crystal, the sum of the pure magnetic and nuclear scattering terms equals the negative interference term. Thus, almost no spin-up neutrons are scattered and the crystal can be used as an analyzer [11]. However, that this is only valid for a single magnetic domain state. Full magnetisation of the Heusler crystal is reached above 2 T. It is reasonable to assume the analysing efficiency of the completely magnetised Heusler crystal to be 0.95-0.96 [18]. The black symbols in the Fig. 5 show the measured asymmetry according (1) normalised to P_{An} = 0.96 as function of the field in the magnet, using optimised flipper currents. A constantly high polarization efficiency of above 99% over whole available field region 2-8 T could be demonstrated.

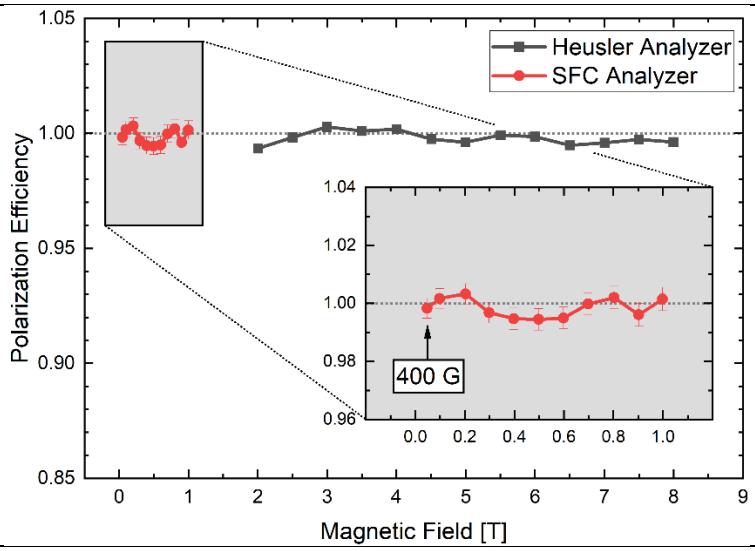

Fig. 5 Experimentally measured polarization efficiency of the new PND setup on POLI. The data are corrected for the analyzing power of the used analyzers (details in the main text). In the low field region (< 1 T), where the Heusler crystal is not fully magnetised, ^{3}He spin filter cell (SFC) was used as an analyzer (red symbols). The Heusler crystal has been used above 2 T (black symbols).

IV CONCLUSION

A new asymmetric field 8 T magnet with large angular access for the scattered neutrons, specially designed to facilitate its application for single crystal neutron diffraction, has been commissioned. With this magnet, a new PND setup has been successfully implemented on the diffractometer POLI at MLZ. In addition to a standard neutron diffractometer, the key components of the new high-field PND option are: supermirror bender polarizer, Mezei-type flipper with dedicated guide field, and the mentioned dedicated magnet. All components were subject to detailed numerical optimisations prior to fabrication. The delivered components were extensively tested and the whole PND setup successfully installed on the beam line. Test experiments show that the new setup provides very high polarization efficiency in the entire available field region and quasi polarization-loss-free transport though the

instrument. This is remarkable especially concerning short wavelength neutrons used on POLI, which request stronger magnetic fields to control precisely the neutron polarization vector in comparison to thermal or cold neutrons. The new high–field PND setup for detailed magnetic structure investigations on POLI is now available for the internal and external user communities via the MLZ proposal system [19].

AKNOWLEDGMENT

H.T. was supported by Tasso Springer Fellowship JCNS FZJ. The instrument POLI is operated by RWTH Aachen University and FZ Jülich (Jülich-Aachen Research Alliance JARA). The bender polarizer was realised within BMBF Project 05K13PA3.

References:

[1] B. Gillon, " La technique classique du rapport de flipping. Applicationaux aimants moléculaires et aux aimants photo-commutables", Collection SFN, EDP Sciences, vol. 7, p. 13–40, 2007.

[2] J. Jeong, B. Lenz, A. Gukasov, X. Fabreges, A. Sazonov, V. Hutanu, A. Louat, D. Bounoua, C. Martins, S. Biermann, V. Brouet, Y. Sidis, and P. Bourges, “Magnetization Density Distribution of Sr2IrO4: Deviation from a Local j(eff)=1/2 Picture,” *Phys. Rev. Lett.,* vol. 125, no. 9, p. 097202, 2020.

[3] M. Deutsch, B. Gillon, N. Claiser, J. M. Gillet, C. Lecomte, and M. Souhassou, “First spin-resolved electron distributions in crystals from combined polarized neutron and X-ray diffraction experiments,” *IUCRJ,* vol. 1, p. 194-199,, 2014.

[4] A. Gukasov, and P. J. Brown, “Determination of atomic site susceptibility tensors from polarized neutron diffraction data,” *J. Phys.: Condens. Matter,* vol. 14, no. 38, p. 8831-8839, 2002.

[5] B. Lebech, B. D. Rainford, P. J. Brown, and F. A. Wedgwood, “Magnetic Form-Factors of Praseodymium and Neodymium Metals,” *J. Magn. Magn. Mater.,* vol. 14, no. 2-3, p. 298-300, 1979.

[6] C. Wilkinson, D. A. Keen, P. J. Brown, and J. B. Forsyth, “The Neutron Diamagnetic Form-Factor of Graphite,” *J. Phys.: Condens. Matter,* vol. 1, no. 24, p. 3833-3839, 1989.

[7] R. Nathans, S. J. Pickart, H. A. Alperin, and P. J. Brown, “Polarized-Neutron Study of Hematite,” *Physical Review a-General Physics,* vol. 136, no. 6a, p. 1641, 1964.

[8] Y. B. Ke, S. Lan, Y. Wu, H. H. Wu, V. Hutanu, H. Deng, A. Pramanick, Y. Ren, and X. L. Wang, “Unraveling magneto-structural coupling of Ni_2MnGa alloy under the application of stress and magnetic field using in situ polarized neutron diffraction,” *Appl. Phys. Lett.,* vol. 117, no. 8, p. 081905, 2020.

[9] H. Thoma, V. Hutanu, H. Deng, V. E. Dmitrienko, P. J. Brown, G. Roth, M. Angst, “Revealing the absolute direction of the Dzyaloshinskii-Moriya interaction in prototypical weak ferromagnets by polarized neutrons,” *Phys. Rev. X,* vol. 11, p. 011060, 2021.

[10] H. Thoma, H. Deng, G. Roth and V. Hutanu, "Setup for polarized neutron diffraction using a high-T_c superconducting magnet on the instrument POLI at MLZ and its applications." *J. Phys.: Conf. Ser*. vol. 1316, p. 012016, 2019.

[11] H. Thoma, W. Luberstetter, J. Peters and V. Hutanu, “Polarized neutron diffraction using a novel high-T_c superconducting magnet on the single-crystal diffractometer POLI at MLZ,” *J. Appl. Crystallogr.,* vol. 51, no. 1, p. 17-26, 2018.

[12] V. Hutanu, “POLI: Polarised hot neutron diffractometer,” *Journal of Large-Scale Research Facilities,* vol. 1, , p. A16, 2015.

[13]O. Kirichek, R.B.E. Down, G. Kouzmenko, J. Keeping, D. Bunce, R. Wotherspoon and Z.A. Bowden, "Operation of superconducting magnet with dillution refrigerator insert in zero boil-off regime", *Cryogenics*, vol. 50, p. 666-669, 2010.

[14]A. Eich, M. Holzle, Y. Su, V. Hutanu, R. Georgii, L. Beddrich, and A. Grzechnik, "Clamp cells for high pressure neutron scattering at low temperatures and high magnetic fields at Heinz Maier-Leibnitz Zentrum (MLZ)," *High Press. Res.*, vol. 41, no. 1, p. 88-96, 2020.

[15]www.nanooptics-berlin.com

[16]V. Hutanu, M. Meven, E. Lelièvre-Berna, and G. Heger, "POLI-HeiDi: the New Polarised Neutron Diffractometer at the Hot Source (SR9) at the FRM II – Project Status", *Physica* B, vol. 404, p. 2633–2636, 2009.

[17][V. Hutanu, M. Meven, S. Masalovich, G. Heger, G. Roth, "^{3}He spin filters for spherical neutron polarimetry at the hot neutrons single crystal diffractometer POLI-HEiDi", *J. Phys.: Conf. Ser.* v. 294, p. 012012, 2011.

[18]P. Courtois, "Characterization of Heusler crystals for polarized neutrons monochromators", *Physica* B, v. 267–268, p. 363–366, 1999.

[19]https://ghost.mlz-garching.de